Rock Mechanics and Rock Engineering
https://doi.org/10.1007/s00603-025-04548-y

ORIGINAL PAPER

# Probability of Rock Block Fracturing Upon Impacting a Rock Bed

Álvaro Vergara[1] · Sergio Palma[2,3] · Raúl Fuentes[1]

Received: 20 August 2024 / Accepted: 19 March 2025


## Abstract

This study investigates the mechanical response of rockfall-induced fragmentation by implementing a novel numerical breakage model within a discrete-element framework. The model evaluates the size distribution and breakage probability of rock blocks upon impact, considering key variables such as impact height and initial rock size. The system consists of a rock buffer layer and a freely falling rock block, with irregular geometries incorporated for greater computational realism. Results highlight the strong influence of impact height and rock size ratio on fragmentation, increasing the breakage probability as energy dissipates through the medium. Notably, rock fracture does not always occur instantaneously upon impact but may be delayed by milliseconds as stress propagates through the granular bed. A simple probability model is proposed to estimate the survival rate of rock blocks based on impact height and rock size, demonstrating strong agreement with reported rockfall cases in caving mines. This approach enables back-analysis of rockfall conditions prior to secondary fragmentation, aiding in the understanding of fragment behaviour within the mineral column before extraction. Additionally, the findings contribute to geomechanical risk mitigation by offering insights into rock mass dynamics and energy dissipation mechanisms during impact.

## Highlights

- A new simple breakage probability model is proposed to evaluate the survival rate of a freely falling rock block upon impacting a rock bed.
- The impact height and the size of the rocks have a direct influence on the resulting final size distribution.
- The numerical model recognises breakage as a non-instantaneous phenomenon until the fracture threshold is reached.
- The network of force chains allows the crushable zone exposed to impact to be determined as the energy is distributed through the granular bed.
- Higher impact heights tend to generate single-sized fragments due to the amount of potential energy of the system, reflected in the rotation of the fragmentation curve towards a single cut-off value.

**Keywords** Rockfall fragmentation · Hazards in rock engineering · Rock fracture · Breakage probability · Discrete-element modelling

✉ Álvaro Vergara
alvaro.vergara@rwth-aachen.de

Sergio Palma
sergio.palma@usm.cl

Raúl Fuentes
raul.fuentes@gut.rwth-aachen.de

[1] Institute of Geomechanics and Underground Technology, Faculty of Civil Engineering, RWTH Aachen, Aachen 52074, Germany

[2] Research and Innovation in Mining Group, Department of Mining Engineering, Metallurgy and Materials, Universidad Técnica Federico Santa María, Santiago 8940897, Chile

[3] Complex Fluids Geomechanics Laboratory, Department of Mining Engineering, Metallurgy and Materials, Universidad Técnica Federico Santa María, Santiago 8940897, Chile

Published online: 10 April 2025

## 1 Introduction

Impact-induced rock fragmentation is a physical phenomenon frequently encountered in nature during rockfalls, rockslides, or rock avalanches in mountainous areas (DeBlasio and Crosta 2015), as well as rockbursts and rock mass "caving" in underground environments (Brown 2007). The process basically consists of the release of a large block of rock (or volumes of rock) from the rock mass, which falls freely, impacting either the downstream surface or adjacent surfaces, being subject to fracture depending on the initial conditions of the system (potential energy, rock geometry, surface conditions, etc.), and rock material properties. Due to the natural risk that the impact of rocks involves, both in human life and in infrastructure and facilities, the evaluation and prediction of the characteristics of the impact must be the object of study in the different disciplines that it involves. The objectives of a post-impact fragmentation study may depend on the requirements and characteristics of the analysis system. The conventional rockfall case requires an evaluation of both the run-out distance of the rock fragments and the impact forces exerted by the rock blocks on the downstream surface, primarily to mitigate and reduce the consequences of the rockfall, using protection embankments or shock-absorbing granular bedding (Lambert and Bourrier 2013; Ferrari et al. 2016). However, in deep underground mining, rockfall (caused by the caving of the rock mass or the transfer of material through ore passes) plays an important role in the degree of rock fragmentation obtained, allowing optimisation of the handling of the fragmented material and its subsequent processing, avoiding the need for secondary reductions, or facilitating their mechanical extraction (Hadjigeorgiou and Lessard 2007; Tampier et al. 2021; Ladinig et al. 2022).

Different efforts have been made to complement the impact mechanics quantification and assessment, from in-situ tests, experimental perspectives, numerical proposals to probability theory, they have sought a complete understanding of rock fracture processes and the consequences that this brings. Some researchers have developed a kinematic and dynamic description of rockfalls from in-situ real cases, highlighting the importance of frictional and restitutive components in impact mechanics, as key sources in the dissipation of energy in the system (Pichler et al. 2005; Giacomini et al. 2009; Asteriou et al. 2012; Wyllie 2014). Shen et al. (2017, 2019, 2020) performed numerical simulations for the analysis of the mechanical behaviour of falling rocks against granular soil and flat surfaces, and they determined that the characteristics of fragmentation are highly correlated both to the shape and size of the rock and the impact velocity on the target surface. Wang and Tonon (2011a, 2011b) applied a discrete-element code to simulate the fracture characteristics of rocks with pre-existing discontinuities, concluding that the presence of these induces the formation of large rock fragments, compared to homogeneous rocks. Chang et al. (2024) were based on real cases of rock avalanches to determine the characteristics of the dynamic fragmentation of the system. Their numerical results demonstrate that fracture processes increase rapidly during the first stage of the phenomenon, due to fracture damage and the violent collision of the blocks with the basement. Research on rock-slide avalanches has shown that the degree of impact-induced fragmentation is mainly caused by the high concentration of contact forces in the impact zone, inducing the formation of finer fragments in the immediate vicinity of the impact (DeBlasio and Crosta 2015; Zhao et al. 2018).

In underground mining systems, back-analysis is usually performed to understand the history of the rock mass during caving fragmentation, continually improving mechanical knowledge of the orebody (Annavarapu 2006, 2019). Veltin et al. (2021) presented a numerical study of the fragmentation of rocks due to impact on flat surfaces using a hybrid finite-discrete methodology applied to caving, comparing the roughness and curvature of the surface and the orientation of the rock concerning the impact plane. It can be seen that both the geometry and the orientation of the rock affect the degree of fragmentation obtained. Sánchez et al. (2019) studied the influence of rock size on the dynamics of gravitational flow, inducing the formation of hang-ups and altering the ore volumes of the extraction zones.

Furthermore, rock impact-induced fragmentation has been an attractive development topic in engineering applied not only to the mining industry, but also to the comminution operations in general. Considering that the size distribution directly affects the energy consumption in grinding, several authors have developed models to describe the behaviour of rock fracture under certain impact energy conditions and predict the degree of fragmentation obtained (Vogel and Peukert 2003, 2004; Shi and Kojovic 2007; Tavares 2009).

Despite the above works, there is still a need to understand rock fracture by impact better. Hence, the objective of this paper is to quantify the survival rate and propose a method to assess and explain rock fragmentation when a rock falls onto a rock bed. The proposal is exemplified and demonstrated for cases of rock falls reported in cave mining, but it can be extrapolated to any configuration beyond underground environments.

## 2 Numerical Methods

### 2.1 Impact Breakage Modelling

The discrete element modelling (DEM) is a numerical technique frequently used in various engineering disciplines, applied to solve problems that cover the science of granular materials, rock media, soil mechanics, powder mechanics, among others (Cundall and Strack 1979). This tool treats a particulate system in a discrete manner, where the translation and rotation of each particle are modelled through Newton's second law of motion. The interactions between the particles are evaluated based on the different contact laws between the bodies (Walton and Braun 1986). The normal and tangential forces are integrated explicitly in time to predict the time history response of the material, using an appropriate numerical integration method.

The Fast-Breakage Model (FBM) (Paluszny et al. 2016), as a discrete grain breakage numerical model implemented within the discrete-element framework, allows the instantaneous breakage of a particle once the minimum fracture energy threshold is reached, replacing the particle with progeny fragments formed by irregular polyhedral (Ansys-Inc. 2024). This model applies the breakage theory proposed by Vogel and Peukert (2004) and extended by Shi and Kojovic (2007), based on fracture mechanics models according to their Weibullian behaviour and similarity reasoning of fracture schemes (Rumpf 1973). The latter hypothesizes that different particles have similar breakage patterns if the stored elastic strain energy of the particles multiplied by the initial particle size is constant. The model allows to describe the breakage probability $P(E_{cum})$ of a grain as:

$$P(E_{cum}) = 1 - \exp\left[-SE_{cum}\left(\frac{d_i}{d_{ref}}\right)\right] \tag{1}$$

in which:

$$\begin{aligned} E_{cum} &= E'_{cum} + E - E_{min} \\ E_{min} &= E_{min,ref}\left(\frac{d_i}{d_{ref}}\right) \end{aligned} \tag{2}$$

where $S$ is a measure of the fracture resistance of the material, $E'_{cum}$ is the accumulated energy prior to a stressing event, $E$ the specific impact energy, $d_i$ and $d_{ref}$ the sizes of the impacted and the reference particle, respectively, and $E_{min,ref}$ the minimum impact energy sufficient to cause fracture in a particle of size $d_{ref}$. Thus, when the energy applied to the particle is greater than the fracture energy of the particle, it will break, generating progeny fragments, whose size distribution is obtained from the fracture index $t_{10}$ of the material:

$$t_{10} = A\left\{1 - \exp\left[-SE_{cum}\left(\frac{d_i}{d_{ref}}\right)\right]\right\} \tag{3}$$

where $t_{10}$ is the fineness index that represents the percentage of the initial mass of the particle that will pass through a sieve of 1/10th of the original size $d_i$, and $A$ is a fit parameter that describes the maximum $t_{10}$ for a particle subject to breakage, obtained through calibration in drop-weight tests. The fineness index of the material enables the determination of its size distribution, utilising the incomplete beta function (Barrios et al. 2011):

$$t_n = \frac{100}{\int_0^1 x^{\alpha_n-1}(1-x)^{\beta_n-1}dx}\int_0^{t_{10}} x^{\alpha_n-1}(1-x)^{\beta_n-1}dx \tag{4}$$

where $\alpha_n$ and $\beta_n$ are coefficients of the model. In this way, the model allows the complete description of the grain size distribution knowing the characteristics of the $t_n$-family curves. Figure 1 shows the calculation scheme of the breakage model, as well as the generation of progeny particles after the impact.

The geometry of the progeny fragments created preserves the initial mass and volume and is based on the Laguerre-Voronoi tessellation algorithm (Imai et al. 1985; Du and Gunzburger 2002). This formulation generates a distribution of points in the space from a generator point (contact point between the particles that become in contact), which will form part of the centroids of each generated progeny fragment. Formally, given a convex domain $\Omega \subset \mathbb{R}^3$, $n$ distinct generator points: $x_1, ..., x_i \in \Omega$ and corresponding weights (inversely proportional to impact energy) $w_1, ..., w_n \in \mathbb{R}$, the Laguerre-Voronoi diagram $\{L_i\}_{i=1}^n$ generated by $(x_1, w_1), ..., (x_n, w_n)\ \forall j \in 1, ..., n$ is defined by:

$$L_i = \left\{x \in \Omega : ||x - x_i||^2 - w_i \leq ||x - x_j||^2 - w_j\right\} \tag{5}$$

This algorithm is further characterised by the generation of the smallest fragments in the vicinity close to the contact point, and larger fragments far from this vicinity, more realistically imitating the brittle fracture of rock materials, in addition to preserving both mass and volume.

### 2.2 Geometry and Pre-Analysis Considerations

The discrete geometry of the system to be modelled is represented in Fig. 2, at the instant where the rock block impacts the rock bed. This configuration includes the main rock block, the rock buffering layer, and the air gap (or impact height, defined as the vertical distance between the rock block and the rock bed). The rock bed is modelled as a monodispersed assembly composed of non-cohesive

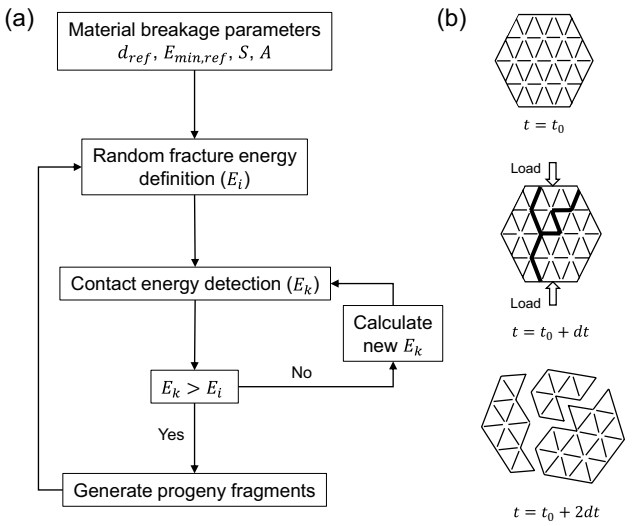


**Fig. 1** **a** Calculation sequence of the instantaneous breakage model. **b** Simplified illustration of the particle breakage process after a stressing event

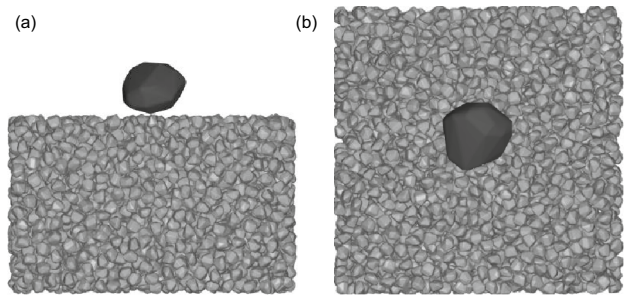


**Fig. 2** Numerical model configuration: **a** front view and **b** top view. The rock block is represented by a single rock (black particle), while the rock bed is represented by a monodisperse assembly of irregularly-shaped particles (gray particles). In this case, $D^* = 5$

irregularly-shaped rocks, with a characteristic size $d$ and randomly oriented. This rock layer is confined by four side walls and one bottom wall to prevent the dispersion of rocks in the system. Its length, width and height dimensions are $50d$. These dimensions were chosen to avoid the influence of the edges of the system within the fracture itself of the rock material, and ensure extensive distribution of energy throughout the medium.

The rock block that falls freely is defined by its characteristic size $D$, and it is the one that impacts the rock bed. Its shape is irregular, as is the buffering layer. Although most numerical studies of granular media assume spherical geometries to represent the discrete bodies, it is well known that the morphological characteristics of the particle directly influences its dynamic and fracture behaviour (Bbosa et al. 2006; Zhu and Zhao 2021). Therefore, the main reason for choosing an irregular geometry is to faithfully represent the mechanics of the rock and avoid simplifications in the fracture process. This geometry is mainly convex, with a smooth and regular outer surface, which facilitates the analysis of stress distribution and crack propagation during the fracture process. The geometry is generated from its fractal dimension as a descriptor parameter of its morphology, well defined in rock materials. This is based on spherical harmonic analysis, which allows controlling the morphology of the particle based on its fractal properties (Wei et al. 2018).

**Table 1** Geometric parameters considered in the numerical model

| Parameter | Value |
|---|---|
| Rock block size, $D$ (m) | [0.1, 0.2, 0.4, 1, 2] |
| Rock size, $d$ (m) | 0.2 |
| Impact height, $h$ (m) | [1, 2, 5, 10, 20, 25] |

For convenience, dimensional analysis will be used to show the main results. The size ratio $D^* \equiv D/d$ is herein defined as the ratio between the size of the rock block $D$ to the size of the rock in the bed $d$. The impact height $h$ has been considered within the common range in rockfalls in underground environments, covering a wide geometric range, i.e. $h = [1\,.\,-\,25\,.]$ m (Galindo-Torres et al. 2018). For this case, the normalised impact velocity $v^* \equiv v_{imp}^2/(gD)$ has been defined as a dimensionless parameter for the analysis of the combined influence of the impact velocity $v_{imp}$ and the size of the rock block $D$ on the system. This parameter is analogous to the square of the Froude number in fluid dynamics, and relates the inertial and gravitational forces acting in the system. Table 1 summarises the combination of geometric variables used in each of the simulations. Based on the table, the ranges of the obtained values are $D^* = [0.5\,.\,-\,10\,.]$, $v_{imp} = [4.429\,.\,-\,22.15\,.]$ m/s, and $v^* = [1\,.\,-\,500\,.]$. The impact velocity $v_{imp}$ is obtained from the conservation of mechanical energy, based on the impact height of the rock block, $v_{imp} = \sqrt{2gh}$.

## 2.3 Calibration of Breakage Properties

The rock material is modelled as low-grade porphyry copper ore, typically exploited by underground caving methods. The use of this type of material to characterise the rock is to subsequently compare the results with those presented in rockfalls in an underground environment. Its fracture properties are obtained through the calibration of single and multiple rocks impact tests based on the experimental works of Jiménez-Herrera et al. (2018) and Barrios et al. (2013, 2020) for the same rock material. The procedure consisted of subjecting particles contained in the size range between 6.3 and

4.75 mm to impact fracture. A steel ball with a diameter of 88 mm and a mass of 2.78 kg was used in the procedure. The impact energy was controlled by varying the impact height, resulting in a velocity range between 1 . and 2.5 . m/s. In this study, we consider that the rock does not present discontinuities or internal cracks, so the scale effect of the calibration process follows the assumption that the product between the fracture energy and the size of the rock is always constant (similarity condition).

The estimation of the breakage model parameters is obtained by equating the fracture energy of the rock and adjusting them to the observed breakage probability function (Eq. 1). Figure 3 shows the comparison of the results obtained through numerical modelling, evaluating both the breakage probability of minerals and the size distribution. Table 2 describes both the material and contact parameters during the interaction, as well as the discrete-element model parameters used. The parameters of the incomplete beta function correspond to those reported by Barrios et al. (2011) for this type of material, which were applied in the calibration process of the numerical model.

Once the mechanical parameters of the material are obtained, the model is validated against a real rockfall case reported by Ruíz-Carulla and Corominas (2020) for the same type of material. This phenomenon involves the impact of three rock blocks (In-Situ Block Size Distribution, IBSD), resulting in the formation of 48 fragments (Rock Block Size Distribution, RBSD) (see Table 3). Figure 4 presents the comparison between the actual and estimated number of blocks as a function of their different volumes. Although the validation process shows good performance of the numerical model against real data, it is important to note that it has output limitations, mainly due to computational time constraints. These restrictions limit the minimum fragment size produced by the model, which has been set to 5% of the initial rock size. This constraint forces a reduction in the model's accuracy when estimating the finer fragments generated after impact.

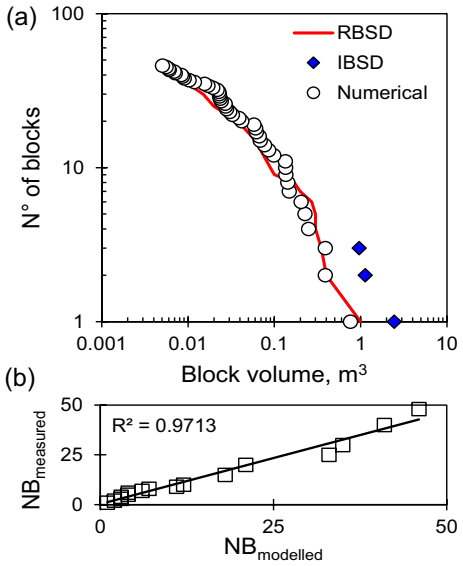


**Fig. 4** Validation of the material's breakage parameters against a real reported rockfall case (Ruíz-Carulla and Corominas 2020). **a** Number of blocks as a function of their volume after impact. The blue markers represent the three initial impactor blocks (IBSD). **b** Comparison between the measured number of blocks and the number of blocks obtained through numerical simulation

During the simulation, the rock buffering layer is deposited randomly oriented at the base applying the gravitational condition until it is at rest. Once the system is static ($t$ = 0 s), the rock block is positioned in the centre on the rock layer, and an initial vertical velocity equivalent to the impact

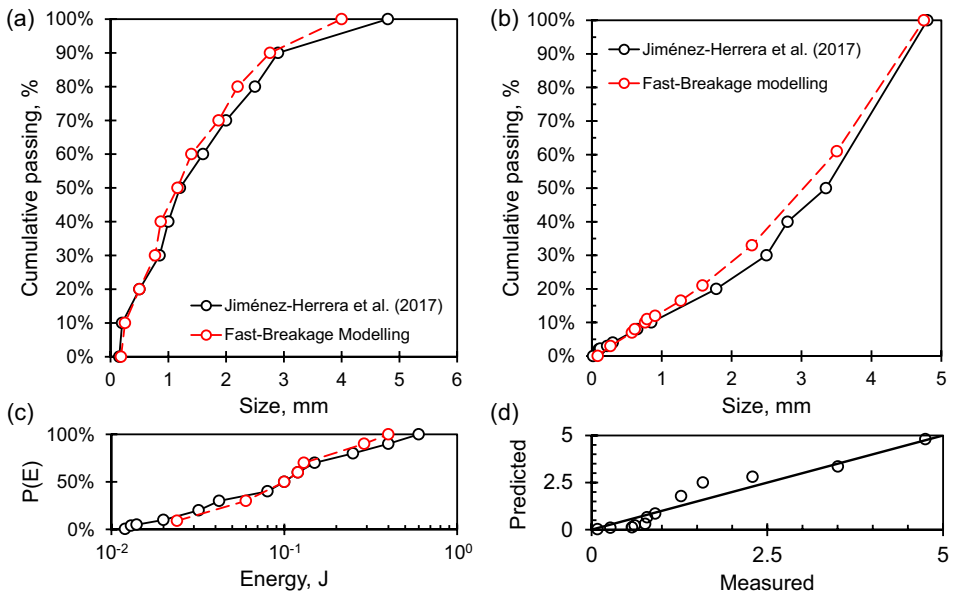


**Fig. 3** Calibration process of the numerical model against the drop-weight tests: **a** Grain size distribution of the single impact breakage test. **b** Grain size distribution of the multiple impact breakage test. **c** Breakage probability of a single specimen versus the applied impact energy. **d** Comparison of the size distribution (in mm) measured by experiments versus that predicted by the numerical model

**Table 2** Elastic and mechanical parameters of the material (low-grade copper ore) used in the model

| Material parameters | |
|---|---|
| Young's Modulus, $E$ (GPa) | 52 . |
| Poisson's ratio, $\nu$ (-) | 0.25 . |
| Density, $\rho$ (kg/m$^3$) | 2930 . |
| Contact parameters (ore-ore) | |
| Coefficient of static friction, $\mu_f$ (-) | 0.59 . |
| Coefficient of restitution, $C_r$ (-) | 0.38 . |
| Breakage model parameters | |
| Reference size, $d_{ref}$ (m) | 0.005 . |
| Minimum specific energy, $E_{min,ref}$ (J/kg) | 100 . |
| Selection function coefficient, $S$ (kg/J) | 0.002 . |
| Maximum $t_{10}$ value, $A$ (-) | 0.67 . |
| Incomplete-beta function coefficients | |
| $\alpha_{1.2}/\beta_{1.2}$. | 0.51 ./11.95 . |
| $\alpha_{1.5}/\beta_{1.5}$. | 1.07 ./13.87 . |
| $\alpha_2/\beta_2$. | 1.01 ./8.09 . |
| $\alpha_4/\beta_4$. | 1.08 ./3.03 . |
| $\alpha_{25}/\beta_{25}$. | 1.01 ./0.53 . |
| $\alpha_{50}/\beta_{50}$. | 1.03 ./0.36 . |
| $\alpha_{75}/\beta_{75}$. | 1.03 ./0.30 . |

**Table 3** Geometric characteristics of the reported rockfall

| Parameter | Value |
|---|---|
| Total volume RBSD (m$^3$) | 4.2 |
| Total volume IBSD (m$^3$) | 4.2 |
| RBSD n° estimated blocks | 48 |
| RBSD n° measured blocks | 48 |
| Min. measured vol (m$^3$) | 0.0007 |
| Max. measured vol (m$^3$) | 1.1 |
| Impact height (m) | 16.5 |

velocity is applied in the first time-step, depending on the degree of impact height to be modelled. To ensure statistically significant results, as well as to provide robustness and minimise the numerical error of the model, each simulation was run 15–20 times and average values are herein reported. The time-step in each iteration is $10^{-6}$ seconds.

## 3 Results and Discussion

### 3.1 Dynamic Impact Characteristics

Impact mechanics involve the dynamic interaction between the rock block and the rock bed once both come into contact. When the rock block impacts the rock layer, the system may or may not experience breakage. This contact between the rocks allows the distribution and propagation of the impact energy throughout the granular system, where a fraction of this energy is dissipated and/or stored in the surrounding rocks as strain energy. If this energy exceeds the minimum threshold for each rock, the rock will fracture. Otherwise, the rock stores this energy during the process, and as the rock block penetrates, the rock is prone to continue accumulating energy even after impact (Eq. 2). This effect indicates that the fracture of rocks does not necessarily occur instantaneously, but as the energy propagates through the granular medium, the rocks accumulate energy until they experience (or not) fracture (within a time-frame of milliseconds, depending on the initial impact conditions, primarily the characteristics of the cushioning granular medium, due to its energy dissipation mechanism. Figure 5 shows the general fracture scheme, where the rocks in direct contact with the rock block are potential to undergo breakage. However, it can be seen that the rock block does not break at the moment of impact, but rather fractures once it has penetrated the rock layer. In the following sections, the main effects of this phenomenon are discussed and quantified.

One way to visualise the dynamic effect of impact within rock fracture is by analysing the contact force chains in the granular media, assuming that most of the fragmentation occurs along it (DeBlasio and Crosta 2014). At the moment of the impact, the large contact forces are mainly concentrated beneath the rock block, while the small contact forces are distributed near the propagation front within the rock layer. Figure 6 shows its evolution, that is, at the moment of impact the shock force wave propagates radially downward within the granular medium (Fig. 6a–c), which stores such strain energy and controls the propagation of the waves. This loss of force results in a gradual disappearance of the contact force chains in a short time (Fig. 6d) until the system reaches a quasi-static condition. This effect was also observed by the numerical study of Shen et al. (2019). Although the force chains do not allow to determine the quantitative characteristics of fragmentation, they do allow to characterise and describe the distribution of forces during and after the impact, where the potential unstable, weak and fracture-prone areas of influence can be determined once these forces exceed the admissible limit of each rock, and even determine the geometric characteristics of the rock shed to reduce the impact of the free-falling rock.

### 3.2 Effect of the Impact Height and Rock Size

The analysis below relies on the breakage probability of the rock block, which depends on the impact energy received by the rock system during interaction. This probability can be understood as the ratio between the number of times a single

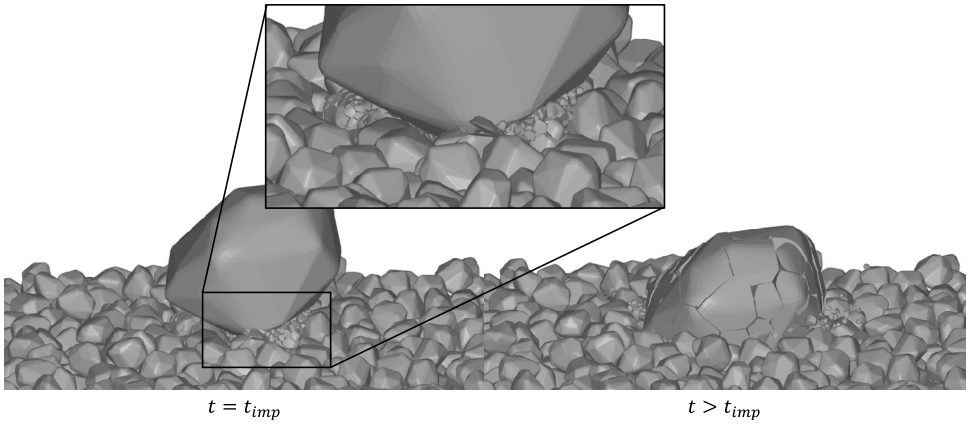


**Fig. 5** Impact fracture diagram. Note that the fracture of the rock block does not necessarily occur at the moment of impact $t = t_{imp}$, but rather in a short period afterwards, when it reaches its fracture energy

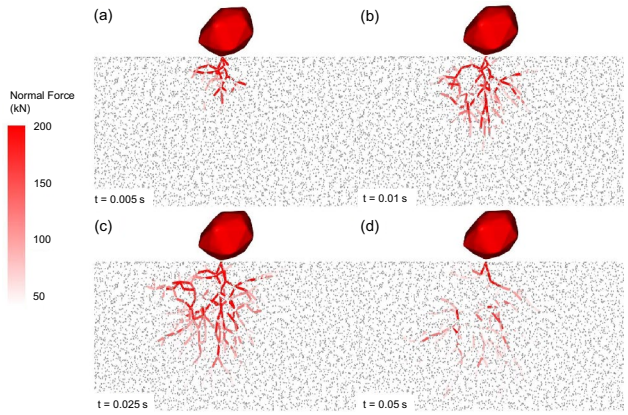


**Fig. 6** Evolution of contact force chains between the rock block and the rock buffer layer with $D^* = 5$ and $h = 15$ m

rock block undergoes fracture over the number of impacts (as a survival quotient).

Figure 7a shows the breakage probability $P(v^*)$ of the rock block as a function of the normalised impact velocity $v^*$, for different size ratios $D^*$.

First, the curve indicates that, for the same value of $D^*$, as the impact height increases (reflected in $v^*$), the probability that the rock block will fracture is greater. This is because a greater impact height implies a greater accumulation of potential energy (directly proportional to height), which is transformed into kinetic energy as the rock block falls, directly proportional to the square of the impact velocity, and, as a consequence, greater energy available to fracture the system.

On the other hand, if we observe the effect of the size ratio $D^*$, as it increases for the same value of $v^*$, the breakage probability of the rock block increases. This indicates that the size difference between the rock block $D$ and the rock layer $d$ plays a key role in energy dissipation. This is because a layer of smaller rocks may tend to have a denser packing compared to a layer of larger rocks. This packing phenomenon would generate a temporary cushioning during impact, where the energy used for fracture would be greater, compared to loosely packed rock layers, where the energy initially tends to distribute, rearranging the particles in the void spaces and leaving a smaller available fracture energy.

The effect of the rock size can be also seen in Fig. 7b, where the breakage probability of the rock block is plotted against the size ratio, for different impact heights. Additionally, the plot shows the influence of the impact height, where values greater than 20 m imply the imminent fracture of the rock block, regardless of its size.

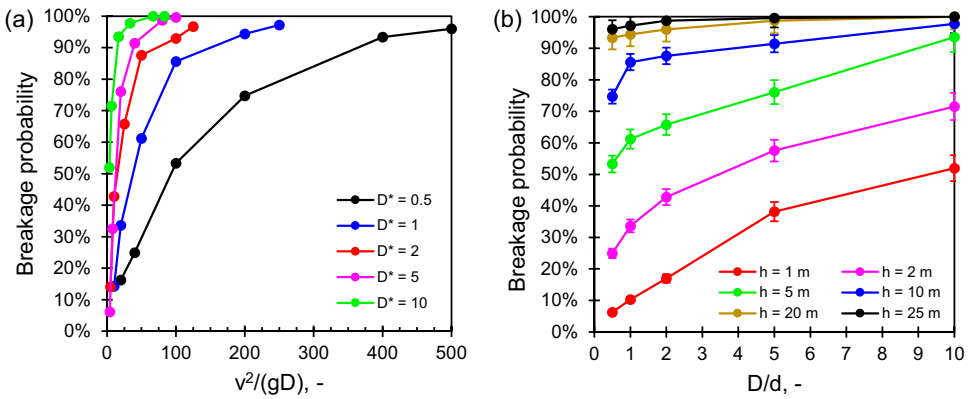


**Fig. 7** Breakage probability of the rock block **a** for different size ratios $D^*$. This probability is plotted against the size ratio for different impact heights, in addition to the error bars representing the standard deviation at each point (**b**)

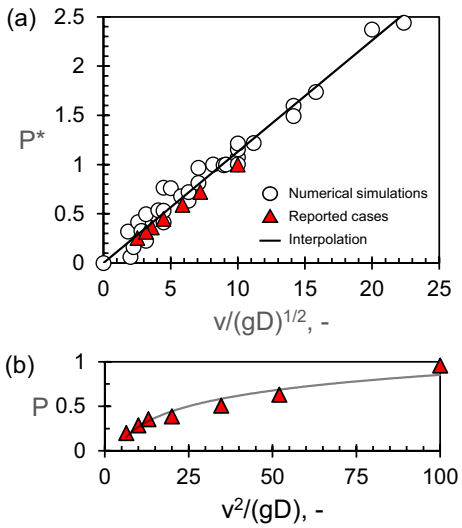


**Fig. 8** **a** Normalised breakage probability $P^*$ against the square root of normalised impact velocity $\sqrt{v^*} = v/\sqrt{gD}$. The circles represent the modelling results, while the triangles correspond to the back-analysis from the reported cases. **b** Breakage probability $P$ as a function of the normalised velocity $v^*$ of the reported cases

Considering the results obtained under the different conditions, the data are adjusted based on the Levenberg-Marquardt regression algorithm (Levenberg 1944). The aim is to propose a simple model that allows estimating the breakage probability of a rock block. Taking this into account, the normalised breakage probability is defined as $P^* \equiv P/[1 - \exp(-D^*)]$, where we hypothesise an exponential behaviour of the breakage probability, considering its Weibullian nature (Weibull 1951). Thus, by plotting this normalised probability $P^*$ as a function of the square root of the normalised impact velocity $\sqrt{v^*}$ (Fig. 8a) and rearranging the equation, the model proposed is obtained:

$$P(h, D, d) = 0.1\sqrt{\frac{2h}{D}}\left[1 - \exp\left(-\frac{D}{d}\right)\right] \tag{6}$$

where $P$ is the breakage probability of the rock block, $h$ the impact height, $D$ the rock block size and $d$ the rock layer size. Thus, the breakage probability of the mineral rock block may be able to estimate knowing the impact height and rock sizes. For cases where the rock layer is not monodisperse, medium size index such as $d_{50}$ can be used.

### 3.3 Fragment Size Distribution and Breakage Quantification

Figure 9a shows the effect of the impact height on the degree of fragmentation of the rock block. The fragment distribution curve allows this effect to be quantified, where it is possible to determine the greater formation of fine particles at higher impact heights. Considering that the impact energy is larger, this is well reflected in the result of the impact through the greater fragmentation of the rock block, where it is important to highlight that the idea of fragmentation in caving is to generate an optimal size of the mineral, whether for the geomechanical control of the caving, as well as for its mechanical handling after extraction. Therefore, the presence of fines, although it can facilitate the gravitational flow of the mineral inhibits the fragmentation process, reducing the impact of fragmentation by functioning as a "cushioning" within the mineral column.

Another important point is the scale-by-size effect. Figure 9b shows this effect for $D^* = 5$ . and an impact height $h = 10$ m. It is observed that despite the irregularity of the applied geometries, there is a pattern in the shape of the size distribution curve, which would be related to how the tessellation algorithm generates the fragments, based purely on energy conditions of the system. Based on the effective diameters in Fig. 9b, the degree of uniformity of the three curves can be determined, obtaining values of: 1.61 ., 1.54 . and 1.56 . for rock block size 0.5 m, 1 m and 2 m, respectively. At this point, it is also important to emphasise that, due to the optimisation of computational resources, the minimum sizes created by the numerical

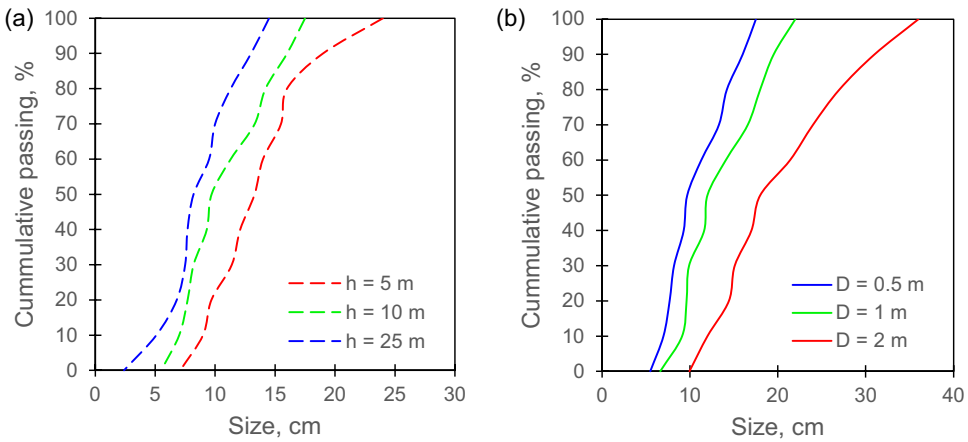


**Fig. 9** **a** Influence of the air gap height on the fragment size distribution for $D = 0.5$ m; and **b** Rock block size effect on the size distribution with $h = 10$ m

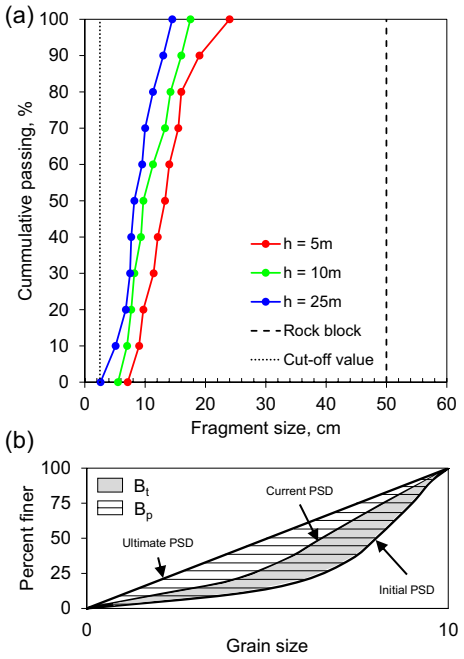


**Fig. 10** **a** Rock block fragmentation curves (based on Fig. 9a); and **b** Definition of the breakage index (Einav 2007)

model were not less than 5% of the initial size of the rock, so values lower than such limit are ignored.

To quantify the degree of fragmentation of the rock block once the impact has occurred, the definition proposed by Einav (2007) will be used, based on the relative position of the fragmentation curve obtained, with respect to the initial size of the rock and an arbitrary cut-off value (in this case, 5% of the initial size, as shown in Fig. 10a). This relative breakage is calculated as an area ratio between the distribution curves. In other words, the potential breakage $B_p$ is the area between the initial and final distribution curves (maximum possible breakage), while the total breakage $B_t$ corresponds to the area enclosed by the initial and current curves. Finally, the relative breakage $B_r$ is defined as: $B_r = B_t/B_p$ (Fig. 10b). Thus, for the different impact heights of 5, 10 and 25 m, relative breakage of 76.7%, 82.5% and 86.8% are obtained, respectively, which represents the influence of the height of the rock fall on its breakage percentage, where at higher heights, the impact will generate mono-sized fragments that tend to the minimum acceptable size (arbitrary cut-off value).

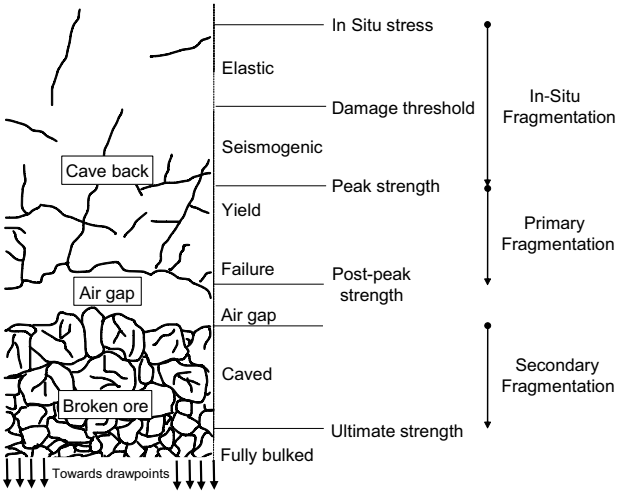


**Fig. 11** Rock mass mechanical response to caving and fragmentation levels recognised in it (modified from Duplancic and Brady 1999)

## 4 Application of the Probability Model to Rockfalls in Caving

Caving mining is an underground method that induces the fragmentation and subsequent collapse of the rock mass, where its early stages are characterised by the impact processes of rocks previously weakened through pre-conditioning techniques (Brown 2007). This breakage process can be understood as a physical phenomenon where a rock block detaches the rock mass and it falls and impacts on a layer of rocks (the muckpile or broken ore), both interacting dynamically. This stage, ignored in many analyses of fragmentation in block caving, has an impact on the size distribution during secondary fragmentation. Figure 11 represents the general scheme of the impact of caving and how the rock mass responds to these dynamic changes.

The validity of Eq. 6 has been tested in a series of cases where the degree of fragmentation has been reported (Table 4). The main objective is to determine the probability based on the reported rock sizes and the air gap. In this way, the breakage probability serves as a back-analysis to deduce and interpret the conditions under which the rockfall occurred (transition between primary and secondary fragmentation). For example, a low breakage probability would indicate an air gap not large enough to produce the desired fragmentation; conversely, a high breakage probability would suggest an air gap sufficiently large to induce a catastrophic impact on mineral fragmentation, resulting in a quantity of fines that reduce secondary fragmentation, and undesirable effects on the dynamic environment of the rock mass (induction of geomechanical risks).

The breakage probability of the reported cases is obtained using Eq. 6, and its results are represented by

**Table 4** Cases of operational underground mines where rockfall is experienced. The reported fragmentation data are used as inputs in Eq. 6, and its results are shown in Fig. 8

| Mine (location) | Description and characteristics | References |
|---|---|---|
| Northern China underground copper mine (China) | Application of Monte Carlo simulations to evaluate the influence of in-situ stress, persistence of discontinuities and rock cohesion on ore fragmentation in block caving | Wang et al. (2003) |
| Deep Ore Zone block caving mine (Indonesia) | Estimation of rock fragmentation based on geotechnics available through drill core mapping and data to optimise the secondary reduction process | Annavarapu (2006) |
| El Teniente mine (Chile) | Analysis of block formation in competent and massive primary copper ore, based on the base structure of the discontinuity network and the formation of blocks during caving | Brzovic and Villaescusa (2007) |
| No reported | A hybrid approach was applied considering the change in the drawpoint fragmentation after the first six months. The stresses and strains estimated using REBOP were used to calculate the effective comminution energies in the movement zones to predict the drawpoint product size distributions | Pierce (2010) |
| Esmeralda mine (Chile) | Size characterisation obtained from the Block Caving Comminution Model for the first 20 m of the mineral extraction column | Gómez et al. (2017) |
| Reservas Norte mine (Chile) | Size characterisation obtained from the Block Caving Comminution Model for the first 20 m of the mineral extraction column | Gómez et al. (2017) |
| Deep Ore Zone block caving mine (Indonesia) | Application of the Block Size Estimator tool to validate primary fragmentation in diorite rock from surface drillings | Annavarapu (2019) |

the red triangles in Fig. 8. These cases are characterised by being deep copper mines (> 500 m), so both the surrounding high-stress system and the high quality of the rock mass have a great influence on the degree of fragmentation and geomechanical phenomena. Although the proposed model depends merely on the geometry of the system, Fig. 8b shows a very good correlation, described by the exponential interpolation. This implies the influence of the geometry of the rock without ignoring its mechanical characteristics, when evaluating the breakage probability in impact systems.

The importance and application of this model in an underground environment allows us to contribute to the evaluation and control of risks associated with air blasts, where large rock blocks fall at high velocity, generating a large impact during the development of the mining project. For example, equation 6 indicates that a greater impact height increases the probability of block fracture, but it should be noted that at the same time a greater air gap increases the possibility of inducing geomechanical hazards inside the mine (as mentioned earlier). Therefore, a good probability of fragmentation could be evaluated from the pre-conditioning of the rock mass, seeking to control the size of the primary blocks that will fall in the first stages of caving.

This interesting finding also allows us to extend the model to the analysis of breakage probability in the control of hazards in rock fall systems. Let us take into account that the idea of generating mitigation barriers can also be understood as a buffer system that allows the fragmentation of falling rocks, with the aim of minimising the effects that a large rock mass can cause in any downstream system. In this case, the control variable is the size $d$ of the rocks that make up the buffer layer, where estimates can predict their optimal design size for the decision to fracture or buffer the rock block in free fall.

## 5 Conclusions

This study has allowed us to quantify the effect of impact-induced fragmentation in rockfalls systems and exemplified to hard rock caving mining in terms of breakage probability, through the application of numerical breakage models in a DEM framework. The numerical model has been validated against experimental tests well reported in the literature, to determine the mechanical properties of the material, to make the fracture process and the size distribution obtained reliable. A set of simulations has been conducted to compare and understand the effect of the impact height and rock sizes on the degree of fragmentation obtained.

The results show a high influence of both the size of the rocks and the impact height on the breakage probability of the system.

A simple probability model has been deduced that compute the breakage probability of the rock block from the geometric conditions of the system, such as the characteristic size of the rocks (both the rock block and the rock layer) and the impact height. This proposed model has been applied to a set of reported fragmentation cases, where exponential interpolation stands out for its good correlation in different rock shapes and sizes in real assessments. This probabilistic model allows a preliminary approximation of the characteristics of said geometries depending on the system and modelling requirements (a high degree of fragmentation is required, as in the case of an underground mining site; or the design of a buffer layer that allows minimising the consequences of the fall of a large block of rock).

In addition, it is important to emphasise both the treatment of the rock shape as an irregular geometry, as well as the use and development of breakage models, giving motivation to the application of this type of system within discrete-element analyses, to obtain more realistic and complete results.

The quantification of the degree of fragmentation shows the effect of the impact height on the generation of the smallest particles, which indicates the importance of monitoring the air gap in underground environments not only for the dynamic control of the rock mass but also to ensure an optimal degree of fragmentation (e.g. improving pre-conditioning techniques prior to mining activity in the rock mass).

Regarding the influence of the impact of the rock block on a rock layer, a potential crushable area is reported, due to the amount of mechanical energy available to be distributed through the contact network in the rock system, which allows the accumulation of strain energy by the rock layer, making it possible to induce its fracture as more rock blocks impact the rock bed during the rockfall process. This scheme supports the prediction of weak or unstable post-impact zones, allowing to determine their influence within the rock layer and how these dynamics can induce geomechanical risks at different levels of underground extraction if they are not controlled, as well as predict the dynamic capacity of protection beds in the evaluation of risk due to rockfalls.

Finally, the proposal of this work provides an alternative tool that contributes to the assessment of the fragmentation process in rockfall systems, caving mining and mine planning, in such a way as to complement the dynamic studies of the rock mass and the influence of fragmentation on the control of risks in natural hazards and geomechanical phenomena in the underground environment.

**Acknowledgements** The author acknowledges the sponsorship of the *Deutscher Akademischer Austauschdienst* (DAAD) and thanks the Dr. D. Wei for providing the Matlab® codes for the generation of the discrete geometries applied in this study.

**Author Contributions** All authors contributed to the study conception and design. Conceptualization, data collection, methodology, material preparation, and formal analysis were performed by Álvaro Vergara. Writing, revision, and editing were supported by Sergio Palma. The project administration, writing, revision and editing, and supervision were guided by Raúl Fuentes.

**Funding** Open Access funding enabled and organized by Projekt DEAL. This work is supported by the National Scientific Research Agency of Chile (ANID): Grant for Doctoral Studies No. 57600326, and Fondecyt Regular Grant No. 1211469.

**Data availability** Data will be made available on request.

## Declarations

**Conflict of interest** The authors have no Conflict of interest.



## References

Annavarapu S (2006) Fragment size estimation and measurement in the doz block cave. Min Eng pp 43–47. https://www.researchgate.net/publication/261833841

Annavarapu S (2019) Field validation of estimated primary fragment size distributions in a block cave mine. J S Afr Inst Min Metall. https://doi.org/10.17159/2411

Ansys-Inc. (2024) Rocky dem technical manual - r1

Asteriou P, Saroglou H, Tsiambaos G (2012) Geotechnical and kinematic parameters affecting the coefficients of restitution for rock fall analysis. Int J Rock Mech Min Sci 54:103–113. https://doi.org/10.1016/j.ijrmms.2012.05.029

Barrios G, Carvalho RD, Tavares L (2011) Modeling breakage of monodispersed particles in unconfined beds. Miner Eng 24:308–318. https://doi.org/10.1016/j.mineng.2010.09.018

Barrios G, de Carvalho R, Kwade A et al (2013) Contact parameter estimation for dem simulation of iron ore pellet handling. Powder Technol 248:84–93. https://doi.org/10.1016/j.powtec.2013.01.063

Barrios G, Jiménez-Herrera N, Tavares L (2020) Simulation of particle bed breakage by slow compression and impact using a dem particle replacement model. Adv Powder Technol 31:2749–2758. https://doi.org/10.1016/j.apt.2020.05.011

Bbosa L, Powell M, Cloete T (2006) An investigation of impact breakage of rocks using the split hopkinson pressure bar. J S Afr Inst Min Metall 106:291–296

Brown ET (2007) Block caving geomechanics, 2nd edn. Julius Kruttschnitt Mineral Research Centre, The University of Queensland, Indooroopilly

Brzovic A, Villaescusa E (2007) Rock mass characterization and assessment of block-forming geological discontinuities during caving of primary copper ore at the El Teniente mine, Chile. Int J Rock Mech Min Sci 44:565–583. https://doi.org/10.1016/j.ijrmms.2006.09.010

Chang W, Xing A, Zhang Y (2024) Dynamic fragmentation characteristics of a heavily jointed rock avalanche: Dem simulation and field seismic signal analysis. Comput Geotech 172:1–17. https://doi.org/10.1016/j.compgeo.2024.106459

Cundall P, Strack D (1979) A discrete numerical model for granular assemblies. Géotechnique 29:47–65. https://doi.org/10.1680/geot.1979.29.1.47

DeBlasio F, Crosta G (2014) Simple physical model for the fragmentation of rock avalanches. Acta Mech 225:243–252. https://doi.org/10.1007/s00707-013-0942-y

DeBlasio F, Crosta G (2015) Fragmentation and boosting of rock falls and rock avalanches. Geophys Res Lett 42:8463–8470. https://doi.org/10.1002/2015GL064723

Du Q, Gunzburger M (2002) Grid generation and optimization based on centroidal Voronoi tessellations. Appl Math Comput 133:591–607. https://doi.org/10.1016/S0096-3003(01)00260-0

Duplancic P, Brady B (1999) Characterisation of caving mechanisms by analysis of seismicity and rock stress. In: Proceedings of the 9th ISRM Congress. International society for rock mechanics, pp 1049–1053

Einav I (2007) Breakage mechanics-part I: Theory. J Mech Phys Solids 55:1274–1297. https://doi.org/10.1016/j.jmps.2006.11.003

Ferrari F, Giacomini A, Thoeni K (2016) Qualitative rockfall hazard assessment: a comprehensive review of current practices. Rock Mech Rock Eng 49:2865–2922. https://doi.org/10.1007/s00603-016-0918-z

Galindo-Torres S, Palma S, Quintero S et al (2018) An airblast hazard simulation engine for block caving sites. Int J Rock Mech Min Sci 107:31–38. https://doi.org/10.1016/j.ijrmms.2018.04.034

Giacomini A, Buzzi O, Renard B et al (2009) Experimental studies on fragmentation of rock falls on impact with rock surfaces. Int J Rock Mech Min Sci 46:708–715. https://doi.org/10.1016/j.ijrmms.2008.09.007

Gómez R, Castro R, Casali A et al (2017) A comminution model for secondary fragmentation assessment for block caving. Rock Mech Rock Eng 50:3073–3084. https://doi.org/10.1007/s00603-017-1267-2

Hadjigeorgiou J, Lessard J (2007) Numerical investigations of ore pass hang-up phenomena. Int J Rock Mech Min Sci 44:820–834. https://doi.org/10.1016/j.ijrmms.2006.12.006

Imai H, Iri M, Murota K (1985) Voronoi diagram in the Laguerre geometry and its applications. SIAM J Comput 14:93–105 (http://www.siam.org/journals/ojsa.php)

Jiménez-Herrera N, Barrios G, Tavares L (2018) Comparison of breakage models in dem in simulating impact on particle beds. Adv Powder Technol 29:692–706. https://doi.org/10.1016/j.apt.2017.12.006

Ladinig T, Wimmer M, Wagner H (2022) Raise caving: a novel mining method for (deep) mass mining. In: Caving 2022. Australian Centre for Geomechanics, pp 651–666. https://doi.org/10.36487/ACG_repo/2205_45

Lambert S, Bourrier F (2013) Design of rockfall protection embankments: a review. Eng Geol 154:77–88. https://doi.org/10.1016/j.enggeo.2012.12.012

Levenberg K (1944) A method for the solution of certain non-linear problemns in least squares. Q Appl Math 2:164–168

Paluszny A, Tang X, Nejati M et al (2016) A direct fragmentation method with Weibull function distribution of sizes based on finite- and discrete element simulations. Int J Solids Struct 80:38–51. https://doi.org/10.1016/j.ijsolstr.2015.10.019

Pichler B, Hellmich C, Mang HA (2005) Impact of rocks onto gravel design and evaluation of experiments. Int J Impact Eng 31:559–578. https://doi.org/10.1016/j.ijimpeng.2004.01.007

Pierce M (2010) A model for gravity flow of fragmentation rock in block caving mines. PhD thesis, The University of Queensland

Ruíz-Carulla R, Corominas J (2020) Analysis of rockfalls by means of a fractal fragmentation model. Rock Mech Rock Eng 53:1433–1455. https://doi.org/10.1007/s00603-019-01987-2

Rumpf H (1973) Physical aspects of comminution and new formulation of a law of comminution. Powder Technol 7:145–159. https://doi.org/10.1016/0032-5910(73)80021-X

Sánchez V, Castro R, Palma S (2019) Gravity flow characterization of fine granular material for block caving. Int J Rock Mech Min Sci 114:24–32. https://doi.org/10.1016/j.ijrmms.2018.12.011

Shen W, Zhao T, Crosta G et al (2017) Analysis of impact-induced rock fragmentation using a discrete element approach. Int J Rock Mech Min Sci 98:33–38. https://doi.org/10.1016/j.ijrmms.2017.07.014

Shen W, Zhao T, Dai F et al (2019) Dem analyses of rock block shape effect on the response of rockfall impact against a soil buffering layer. Eng Geol 249:60–70. https://doi.org/10.1016/j.enggeo.2018.12.011

Shen W, Zhao T, Dai F et al (2020) Discrete element analyses of a realistic-shaped rock block impacting against a soil buffering layer. Rock Mech Rock Eng 53:3807–3822. https://doi.org/10.1007/s00603-020-02116-0

Shi F, Kojovic T (2007) Validation of a model for impact breakage incorporating particle size effect. Int J Miner Process 82:156–163. https://doi.org/10.1016/j.minpro.2006.09.006

Tampier C, Mascaró M, del Solar JR (2021) Autonomous loading system for load-haul-dump (lhd) machines used in underground mining. Appl Sci 11:8718. https://doi.org/10.3390/app11188718

Tavares L (2009) Analysis of particle fracture by repeated stressing as damage accumulation. Powder Technol 190:327–339. https://doi.org/10.1016/j.powtec.2008.08.011

Veltin K, Elmo D, Rogers S (2021) A hybrid fem/dem approach to estimating rock block breakage due to gravity free-fall. In: IOP Conference Series: Earth and Environmental Science, vol 833. IOP Publishing Ltd, doi: https://doi.org/10.1088/1755-1315/833/1/012098

Vogel L, Peukert W (2003) Breakage behaviour of different materials-construction of a mastercurve for the breakage probability. Powder Technol 129:101–110 (www.elsevier.com/locate/powtec)

Vogel L, Peukert W (2004) Determination of material properties relevant to grinding by practicable labscale milling tests. Int J Miner Process 74:329–338. https://doi.org/10.1016/j.minpro.2004.07.018

Walton O, Braun R (1986) Viscosity, granular-temperature, and stress calculations for shearing assemblies of inelastic, frictional disks. J Rheol 30:949–980. https://doi.org/10.1122/1.549893

Wang Y, Tonon F (2011) Discrete element modeling of rock fragmentation upon impact in rock fall analysis. Rock Mech Rock Eng 44:23–35. https://doi.org/10.1007/s00603-010-0110-9

Wang Y, Tonon F (2011) Dynamic validation of a discrete element code in modeling rock fragmentation. Int J Rock Mech Min Sci 48:535–545. https://doi.org/10.1016/j.ijrmms.2011.02.003

Wang L, Yamashita S, Sugimoto F et al (2003) A methodology for predicting the in situ size and shape distribution of rock blocks. Rock Mech Rock Eng 36:121–142. https://doi.org/10.1007/s00603-002-0039-8

Wei D, Wang J, Nie J et al (2018) Generation of realistic sand particles with fractal nature using an improved spherical harmonic analysis. Comput Geotech 104:1–12. https://doi.org/10.1016/j.compgeo.2018.08.002

Weibull W (1951) A statistical distribution function of wide applicability. J Appl Mech https://hal.archives-ouvertes.fr/hal-03112318

Wyllie D (2014) Calibration of rock fall modeling parameters. Int J Rock Mech Min Sci 67:170–180. https://doi.org/10.1016/j.ijrmms.2013.10.002

Zhao T, Crosta G, Dattola G et al (2018) Dynamic fragmentation of jointed rock blocks during rockslideavalanches: insights from discrete element analyses. J Geophys Res: Solid Earth 123:3250–3269. https://doi.org/10.1002/2017JB015210

Zhu F, Zhao J (2021) Interplays between particle shape and particle breakage in confined continuous crushing of granular media. Powder Technol 378:455–467. https://doi.org/10.1016/j.powtec.2020.10.020